Science Advances
AAAS

Supplementary Materials for

Nanoengineered mesenchymal stem cell therapy for pulmonary fibrosis in young and aged mice

Meng-Meng Han *et al.*

Corresponding author: Hu-Lin Jiang, jianghulin3@gmail.com

jianghulin3@163.com

Sci. Adv. **9**, eadg5358 (2023)
DOI: 10.1126/sciadv.adg5358

This PDF file includes:

Supplementary Figures

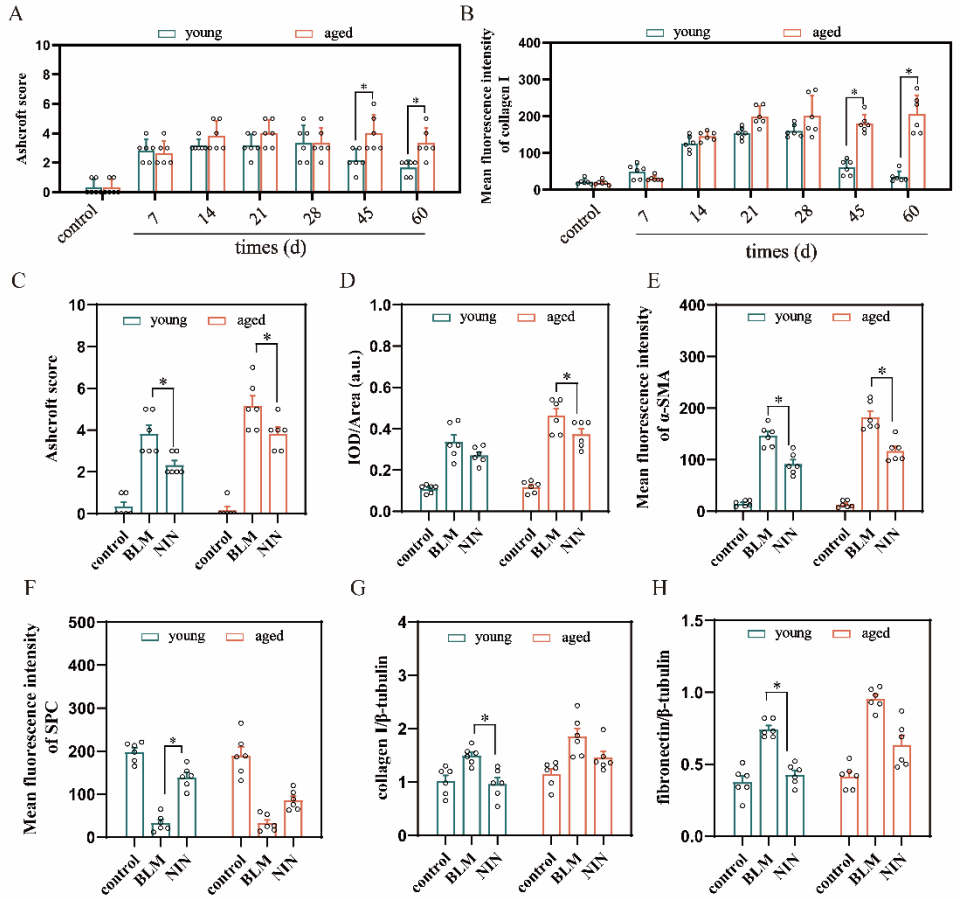

Fig. S1. PF progression in young and aged mice. Ashcroft score (**A**) and quantitative results of IF of collagen I (**B**) on young and aged mice challenged with BLM for different times. Ashcroft score (**C**) and integrated optical density (IOD) per area of Masson staining (**D**) of the lungs of young and aged mice treated with NIN. Mean fluorescence intensity of α-SMA (**E**) and SPC (**F**). WB quantitative analysis of collagen I (**G**) and fibronectin (**H**). Data are mean ± SD. *$P < 0.05$.

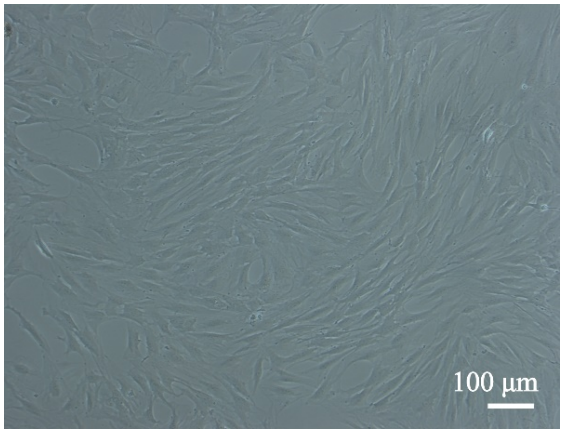

Fig. S2. The morphologies of MSCs. The morphology of the MSCs was fusiform.

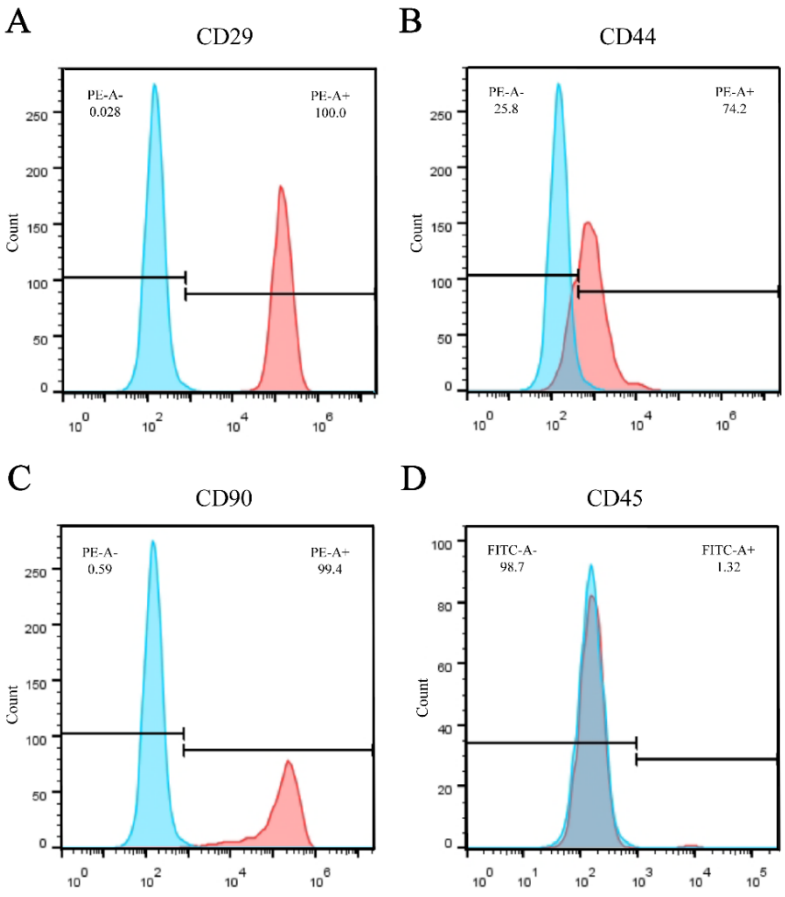

Fig. S3. The identification of MSCs surface markers. (**A**) CD29. (**B**) CD44. (**C**) CD90. (**D**) CD45.

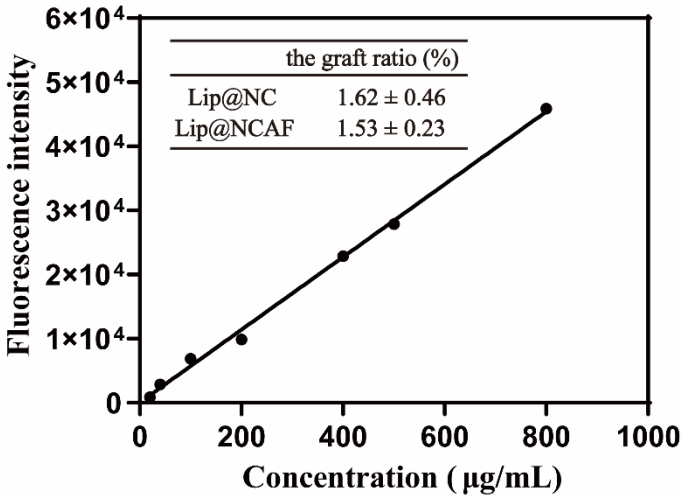

Fig. S4. The quantification of type I collagenase attached on Lip@NC and Lip@NCAF. Type I collagenase quantification. Standard curve of FITC in the supernatant (Ex: 485 nm, Em: 530 nm) (n=5). Data are means ± S.D.

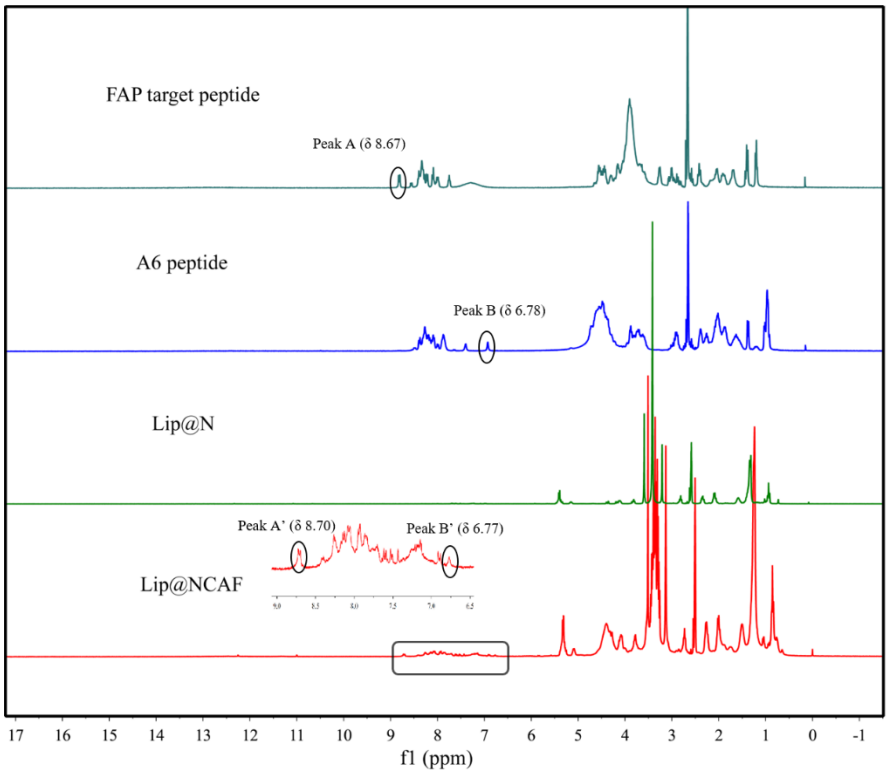

Fig. S5. The characterization of Lip@NCAF. ^{1}H-NMR spectra of FAP target peptide, A6 peptide, Lip@N and Lip@NCAF, respectively.

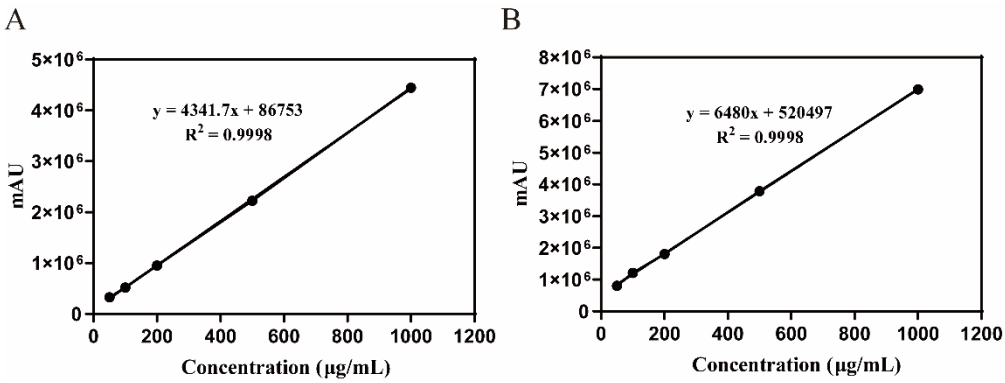

Fig. S6. The graft ratios of A6 peptide and FAP target peptide. Standard curve of A6 peptide (**A**) and FAP target peptide (**B**).

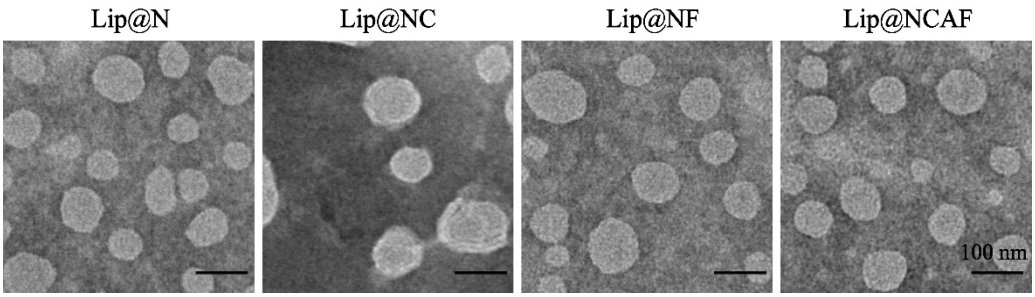

Fig. S7. The micromorphology of different formulations. TEM photographs of Lip@N, Lip@NC, Lip@NF and Lip@NCAF, respectively.

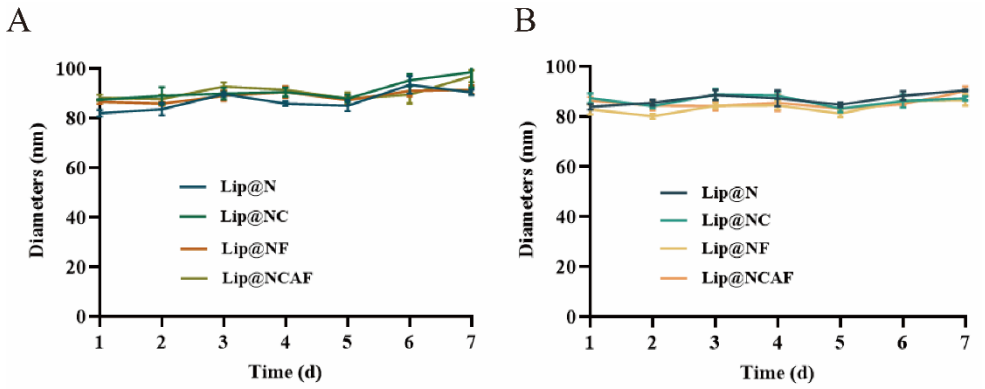

Fig. S8. The stability of different formulations. The particle size changes of Lip@N, Lip@NC, Lip@NF and Lip@NCAF in PBS (**A**) and DMEM containing 10% FBS (**B**) (n=5). Data are mean ± S.D.

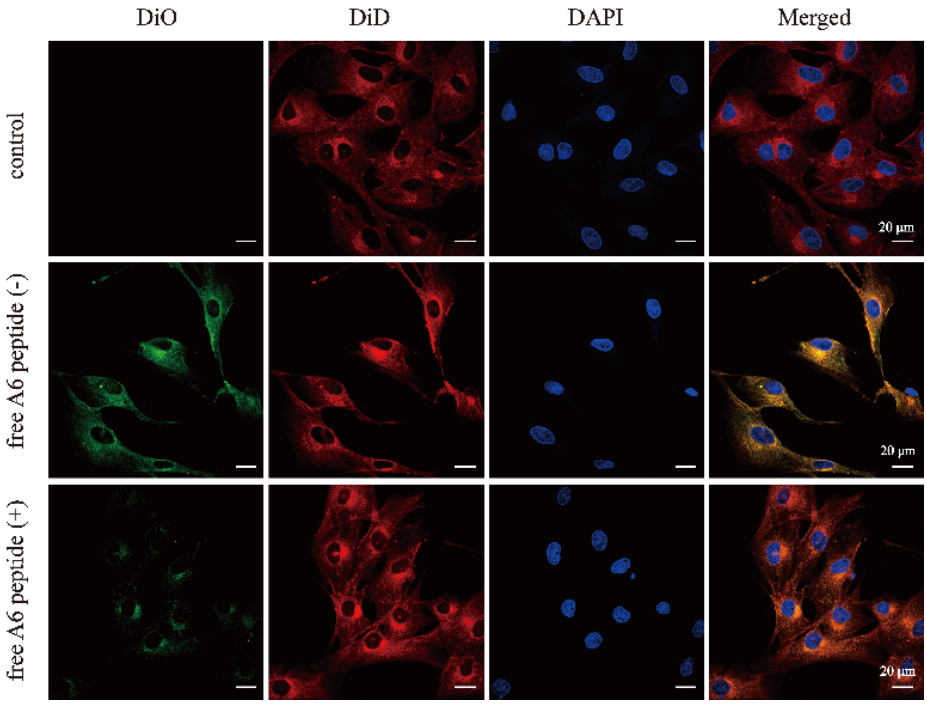

Fig. S9. The combination mechanism of MSCs and Lip@NCAF. CLSM images of DiD-labeled MSCs incubated with DiO-labeled Lip@CAF in the presence or absence of free A6 peptide preincubation.

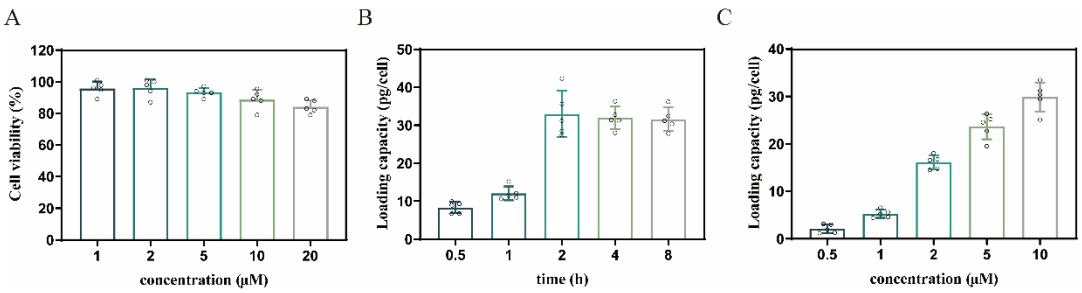

Fig. S10. The cell viability and loading capacity of MSCs. Cell viability of MSCs (**A**) treated with different concentrations of Lip@NCAF. The loading capacity of MSCs incubated with Lip@NCAF for different times (**B**) and at different concentrations (**C**) (n=5). Data are mean ± S.D.

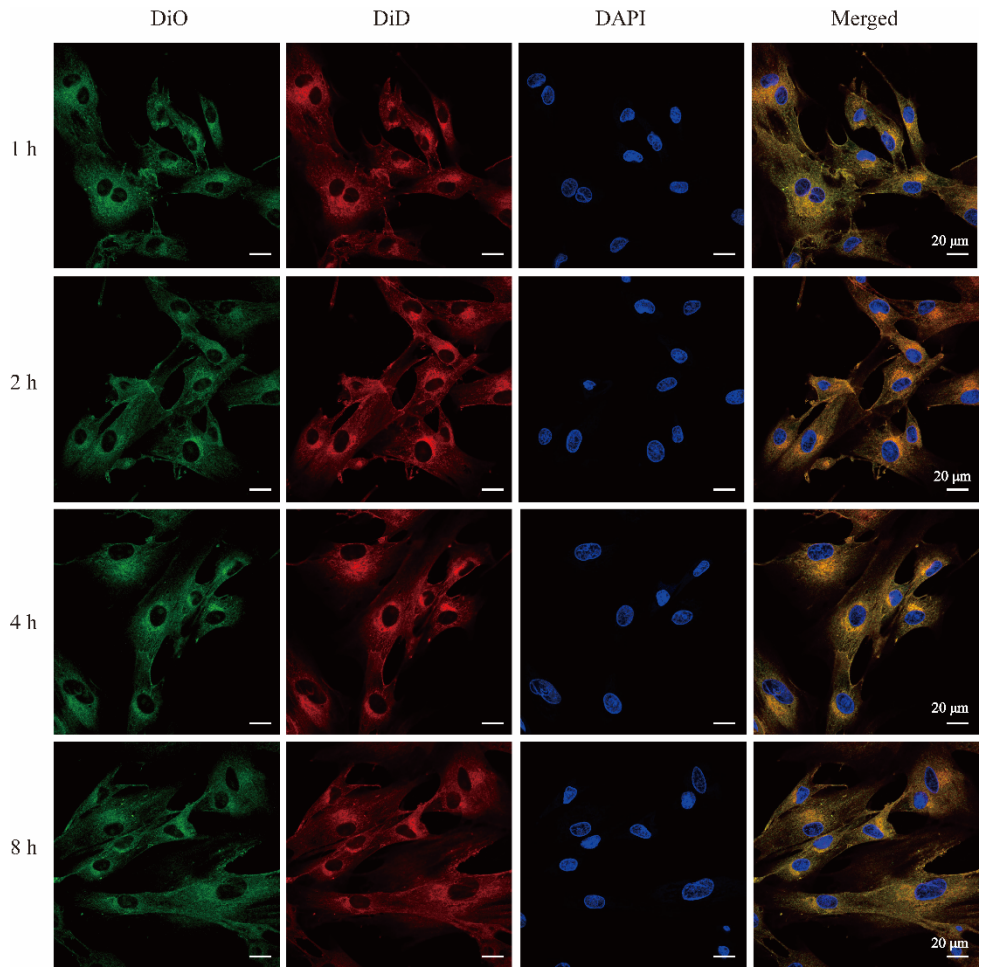

Fig. S11. The time-dependent combination of MSCs and Lip@NCAF. CLSM images of DiD-labeled MSCs incubated with DiO-labeled Lip@CAF for 1 h, 2 h, 4 h and 8 h, respectively.

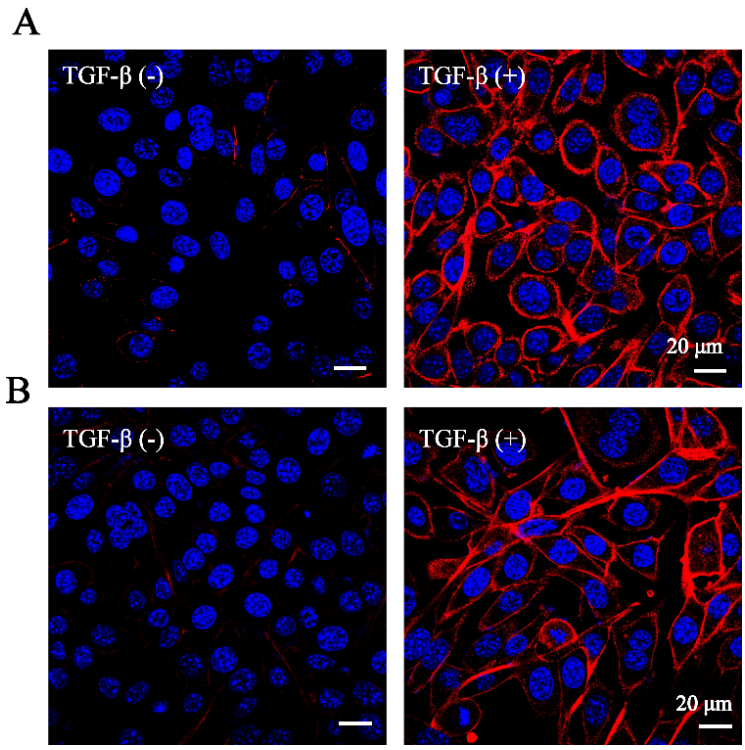

Fig. S12. The identification of fibroblasts from young and aged mice. IF staining of α-SMA of y-fibroblasts (**A**) and a-fibroblasts (**B**) treated with TGF-β.

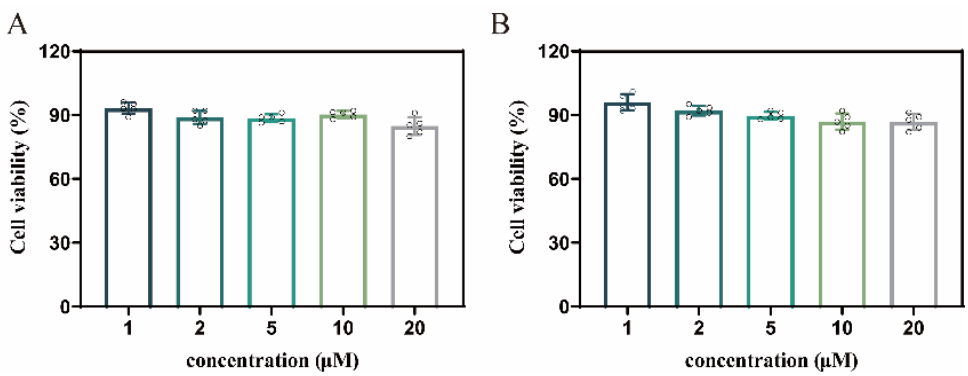

Fig. S13. The viability of fibroblasts after incubation with Lip@NCAF. Cell viability of y-fibroblasts (**A**) and a-fibroblasts (**B**) treated with different concentrations of Lip@NCAF (n=5). Data are mean ± S.D.

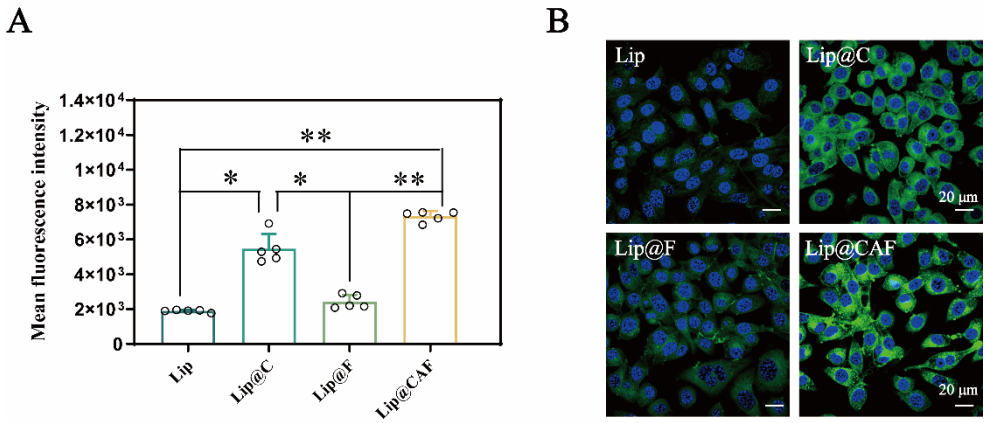

Fig. S14. The uptake of Lip@NCAF by a-fibroblasts. (**A**) The fluorescence intensity of a-fibroblasts was measured by FCM after adding different coumarin 6-labeled formulations to the Transwell chambers. (**B**) Cellular uptake in a-fibroblasts, as shown by CLSM. (n = 5). Data are mean ± S.D. **P* < 0.05 and ***P* < 0.01.

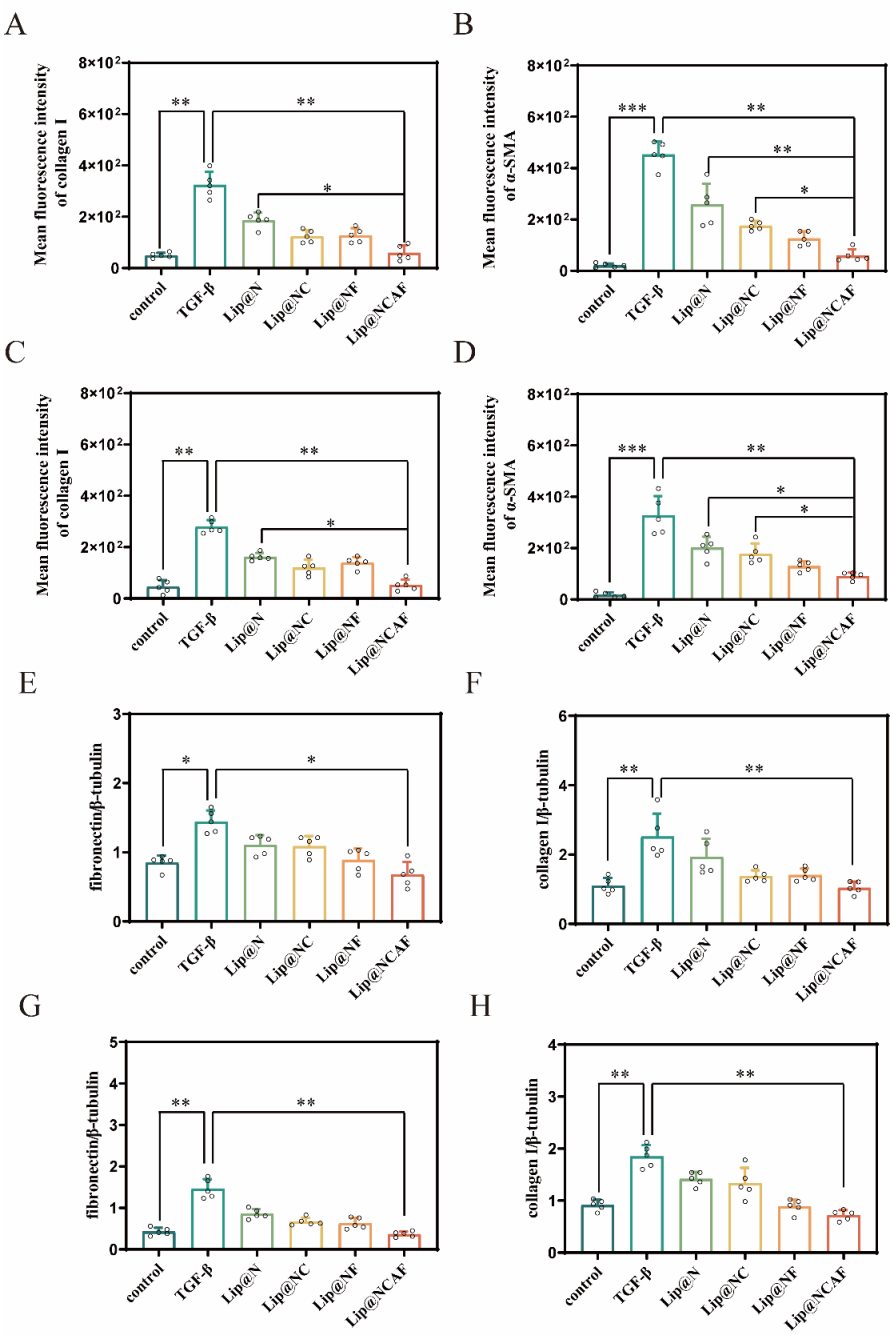

Fig. S15. The antifibrotic effects of MSCs-Lip@NCAF in vitro. Quantitative results of IF staining of collagen I and α-SMA in y-fibroblasts (**A** and **B**) and a-fibroblasts (**C** and **D**). Quantitative results of WB of fibronectin and collagen I in y-fibroblasts (**E** and **F**) and a-fibroblasts (**G** and **H**). (n = 5). Data are mean ± S.D. **P* < 0.05, ***P* < 0.01 and ****P* < 0.001.

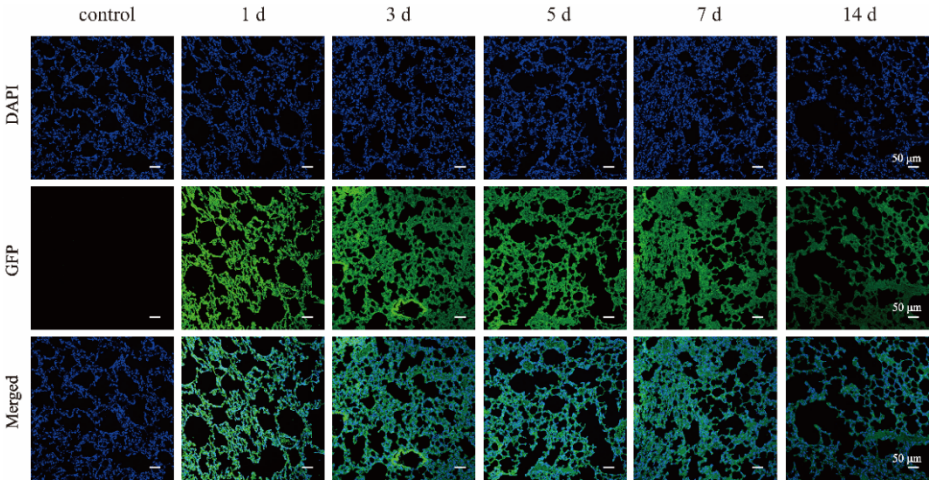

Fig. S16. Lung-targeting ability of MSCs-Lip@NCAF in vivo. CLSM images of lung sections after the mice were injected with MSCs stably expressing GFP.

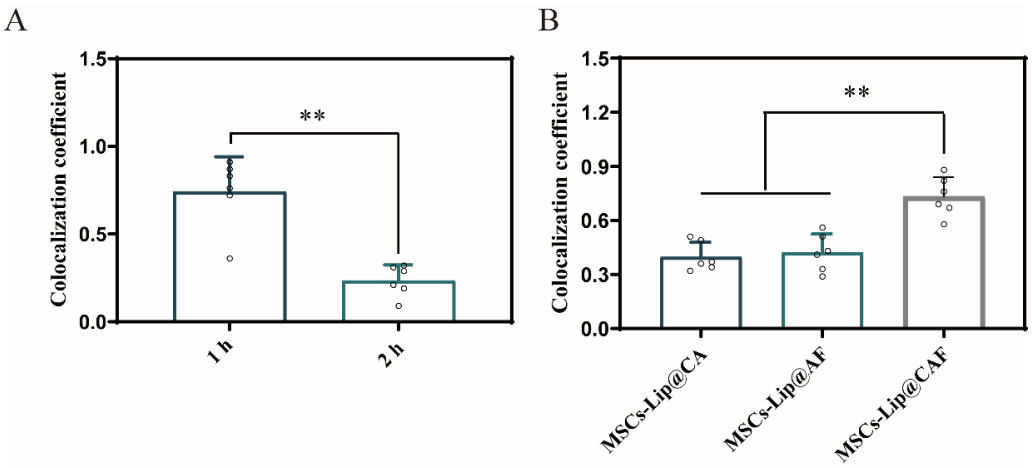

Fig. S17. Behavior of MSCs-Lip@NCAF in vivo. (**A**) Colocalization coefficient of DiI-labeled MSCs and DiO-labeled Lip@CAF after injection for 1 h and 2 h. (**B**) Colocalization coefficient of DiO-labeled Lip@CAF and FAP-positive fibroblasts after 4 h post injection. (n = 6). Data are mean ± S.D. $^{**}P < 0.01$.

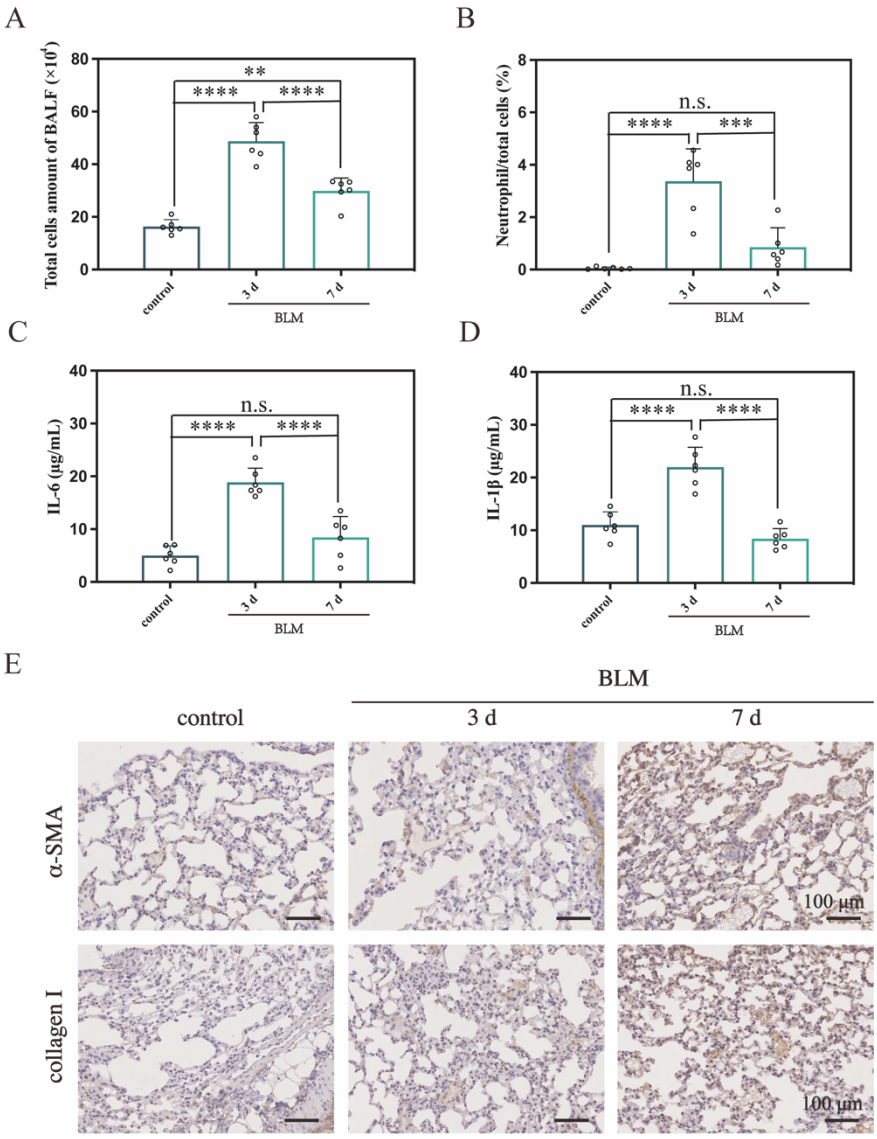

Fig. S18. Inflammation and fibrosis progression after BLM instillation. Total cells amount of bronchoalveolar lavage fluid (BALF) (**A**), the proportion of neutrophils (**B**), the levels of IL-6 (**C**) and IL-1β (**D**) after the young mice were treated with BLM for 3 days and 7 days. (**E**) The expressions of α-SMA and collagen I (n=6). Data are mean ± S.D. $^{**}P < 0.01$, $^{***}P < 0.001$, $^{****}P < 0.0001$ and n.s. no significant difference.

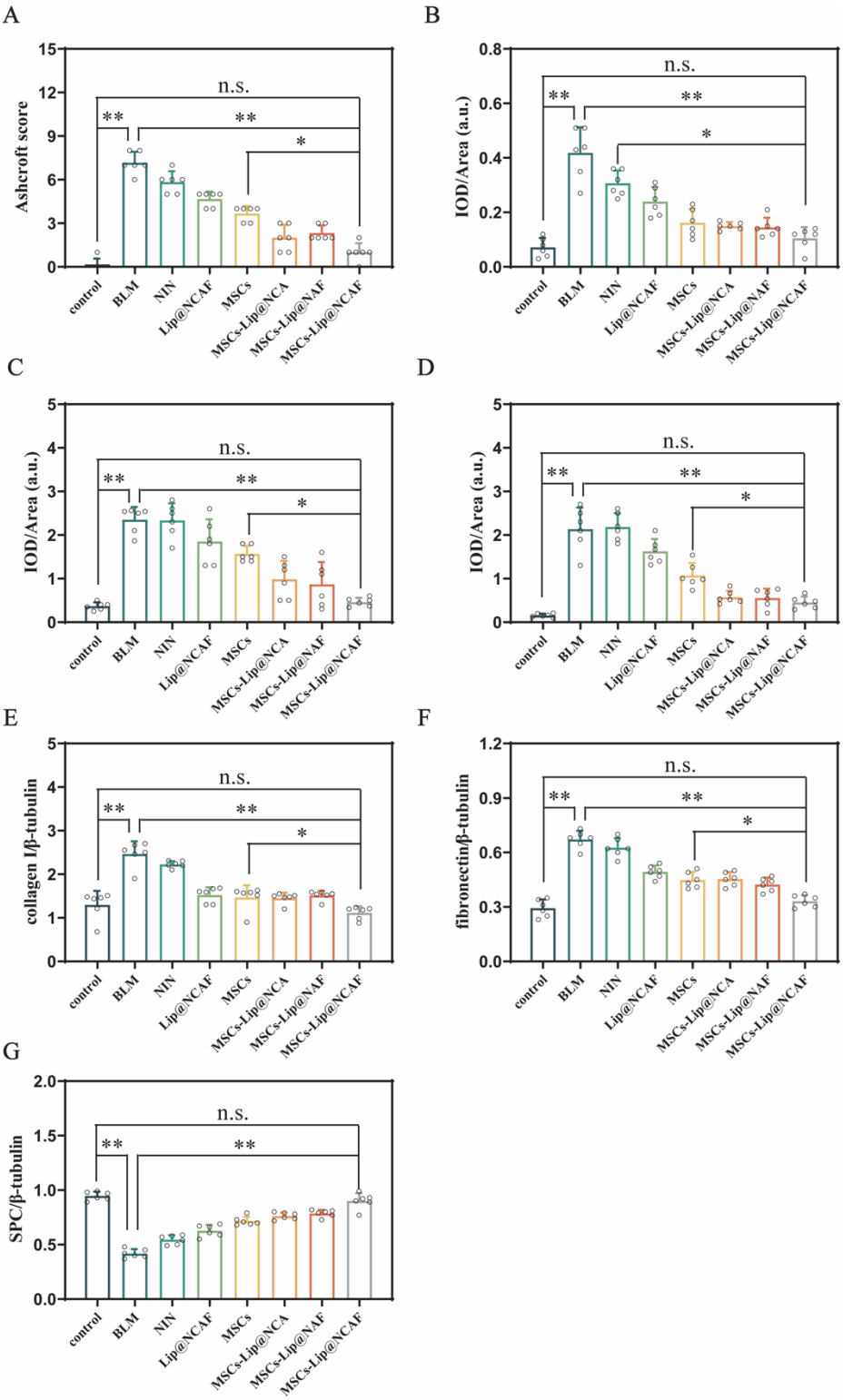

Fig. S19. Antifibrotic effects of MSCs-Lip@NCAF on young mice. Ashcroft score (**A**), IOD/area of Masson staining (**B**), collagen I (**C**) and α-SMA (**D**) of young mice treated with different formulations. WB quantitative analysis of collagen I (**E**), fibronectin (**F**) and SPC (**G**). (n=6). Data are mean ± SD. **P* < 0.05, ***P* < 0.01 and n.s. no significant difference.

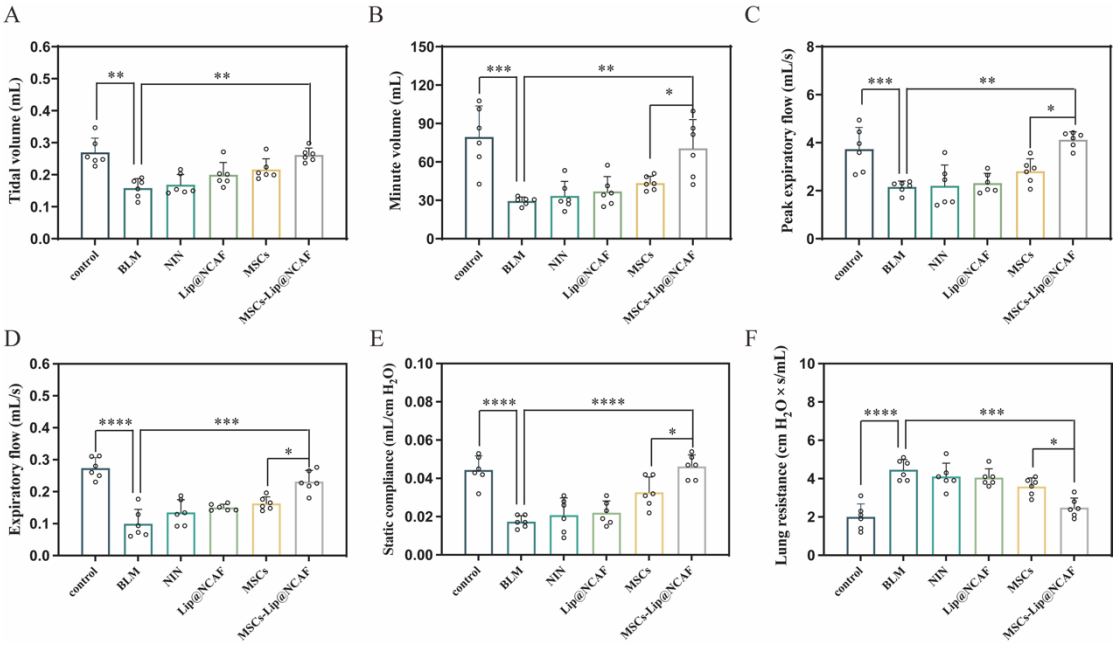

Fig. S20. Lung functional test of the young mice treated with different formulations. Tidal volume (**A**), minute volume (**B**), peak expiratory flow (**C**), expiratory flow 50 (**D**), static compliance (**E**) and lung resistance (**F**) of the young mice treated with NIN, Lip@NCAF, MSCs and MSCs-Lip@NCAF. (n=6). Data are mean ± S.D. **P* < 0.05, ***P* < 0.01, ****P* < 0.001 and *****P* < 0.0001.

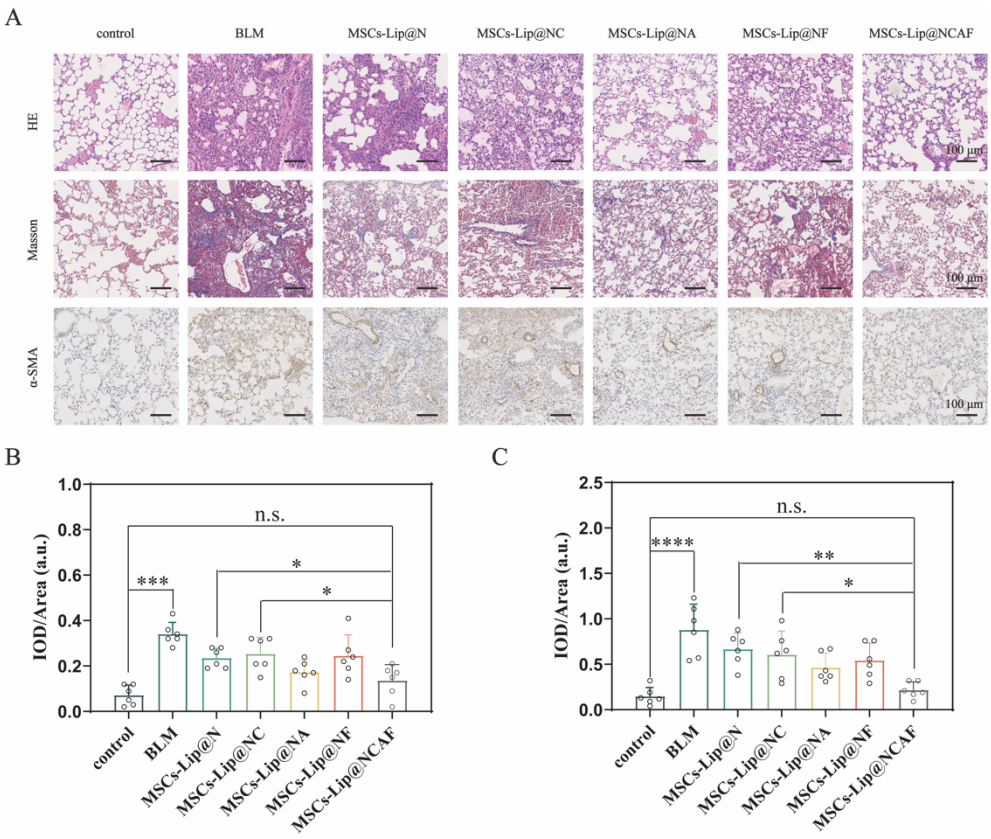

Fig. S21. The antifibrotic effects of type I collagenase, A6 peptide and FAP target peptide. (**A**) HE staining, Masson staining and IHC staining of lung sections from young mice treated with different formulations. Quantitative results of Masson staining (**B**) and α-SMA (**C**). (n=6). Data are mean ± S.D. **P* < 0.05, ***P* < 0.01, ****P* < 0.001, *****P* < 0.0001 and n.s. no significant difference.

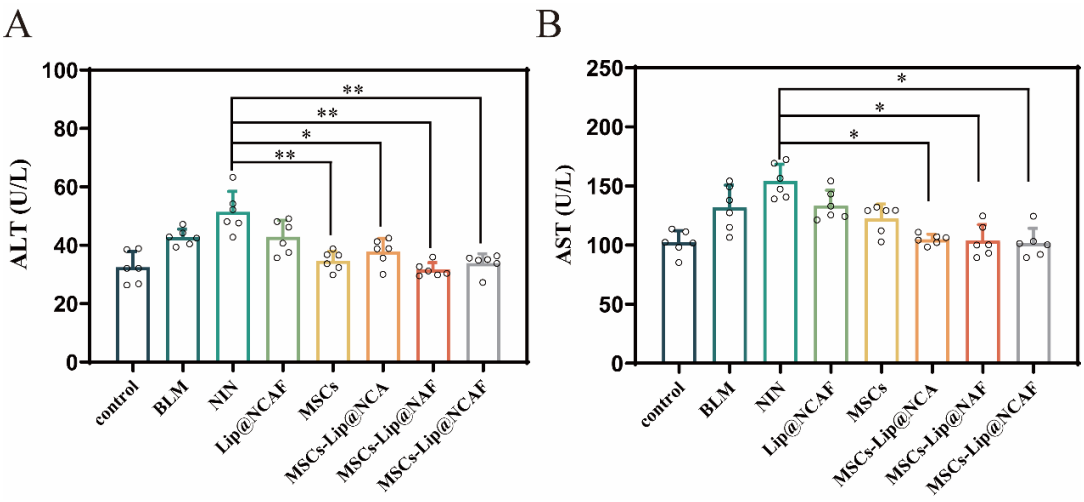

Fig. S22. The levels of ALT and AST of young mice after treated with different formulations. Serum ALT (**A**) and AST (**B**) levels of PF in young mice treated with different formulations for 3 weeks (n=6). Data are mean ± S.D. **P* < 0.05 and ***P* < 0.01.

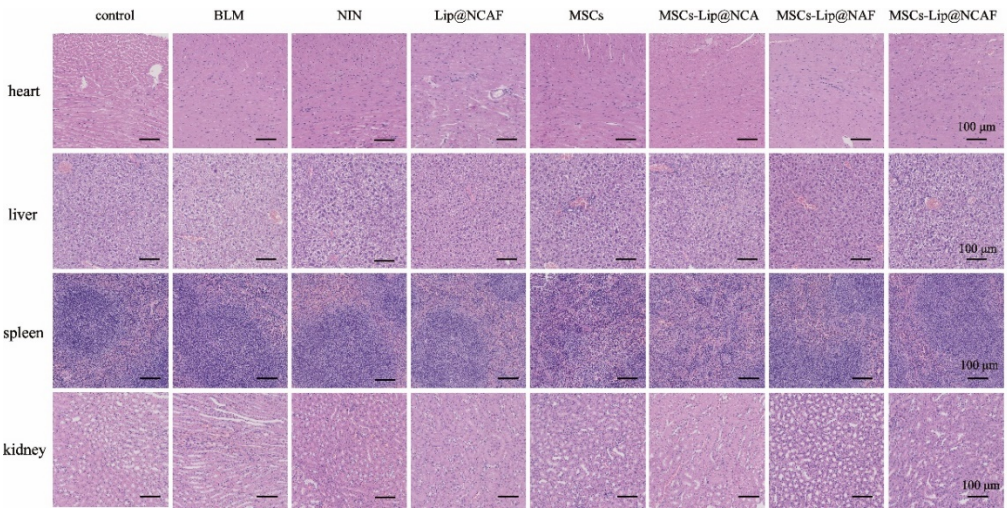

Fig. S23. Systemic toxicity after treated with different formulations. H&E staining of heart, liver, spleen and kidney of PF in young mice treated with different formulations for 3 weeks.

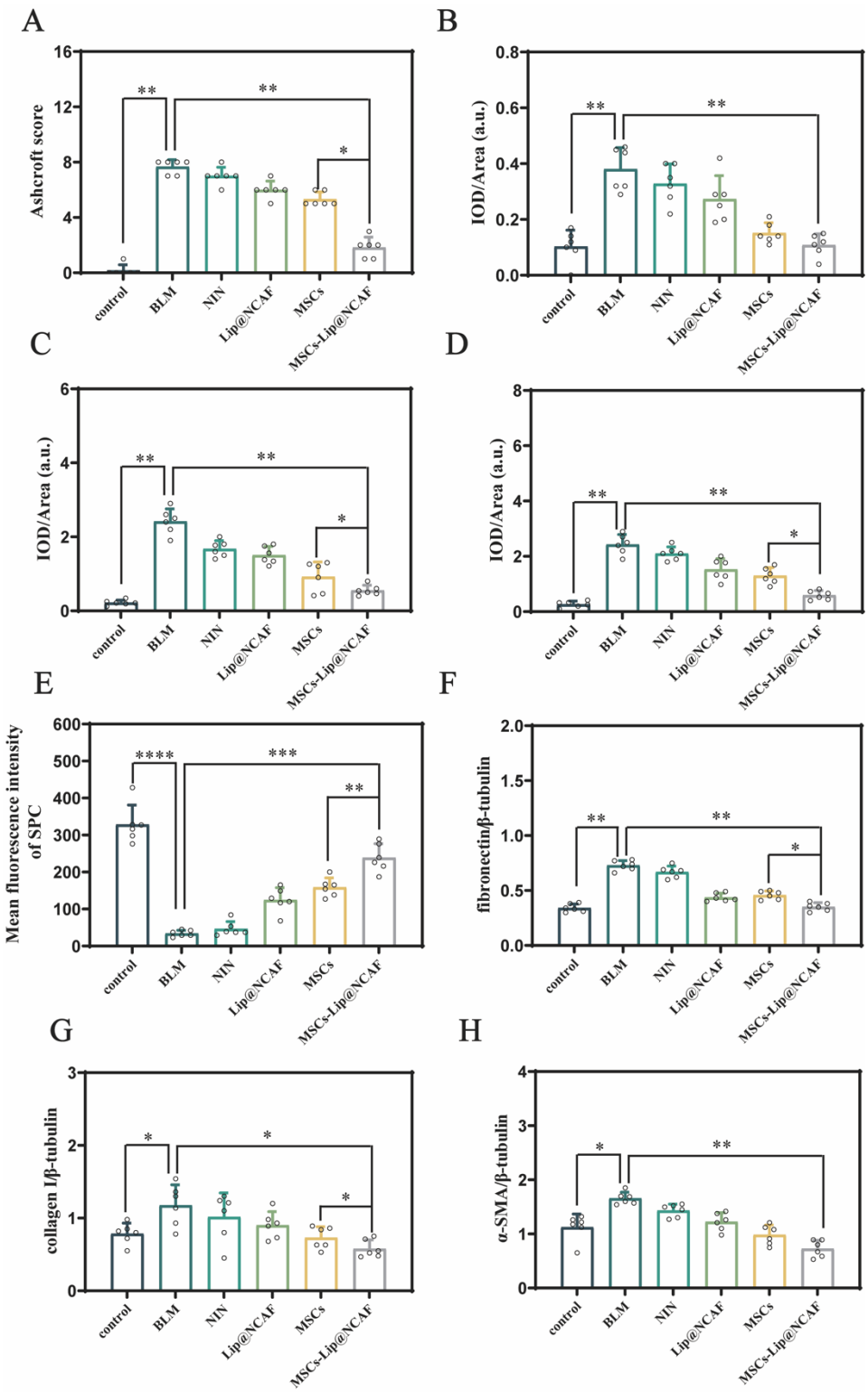

Fig. S24. Antifibrotic effects of MSCs-Lip@NCAF on aged mice. Ashcroft score (**A**), IOD/area of Masson staining (**B**), collagen I (**C**) and α-SMA (**D**), mean fluorescence intensity of SPC (**E**) of the lungs of aged mice treated with different formulations. WB quantitative analysis of fibronectin (**F**), collagen I (**G**) and α-SMA (**H**). (n=6). Data are mean ± SD. *$P < 0.05$, **$P < 0.01$, ***$P < 0.001$ and ****$P < 0.0001$.

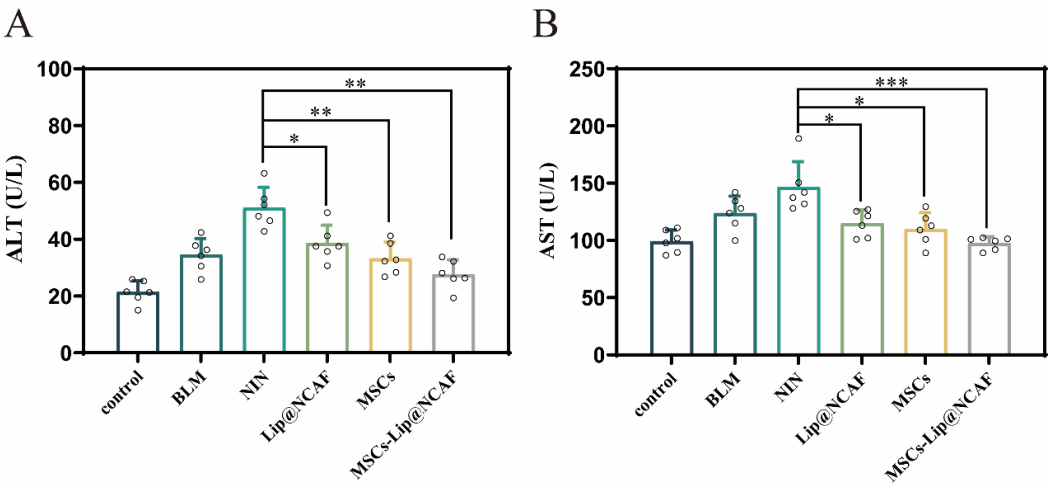

Fig. S25. The levels of ALT and AST of aged mice after treated with different formulations. Serum ALT (**A**) and AST (**B**) levels of PF in aged mice treated with different formulations for 3 weeks (n=6). Data are mean ± S.D. **P* < 0.05, ***P* < 0.01 and ****P* < 0.001.

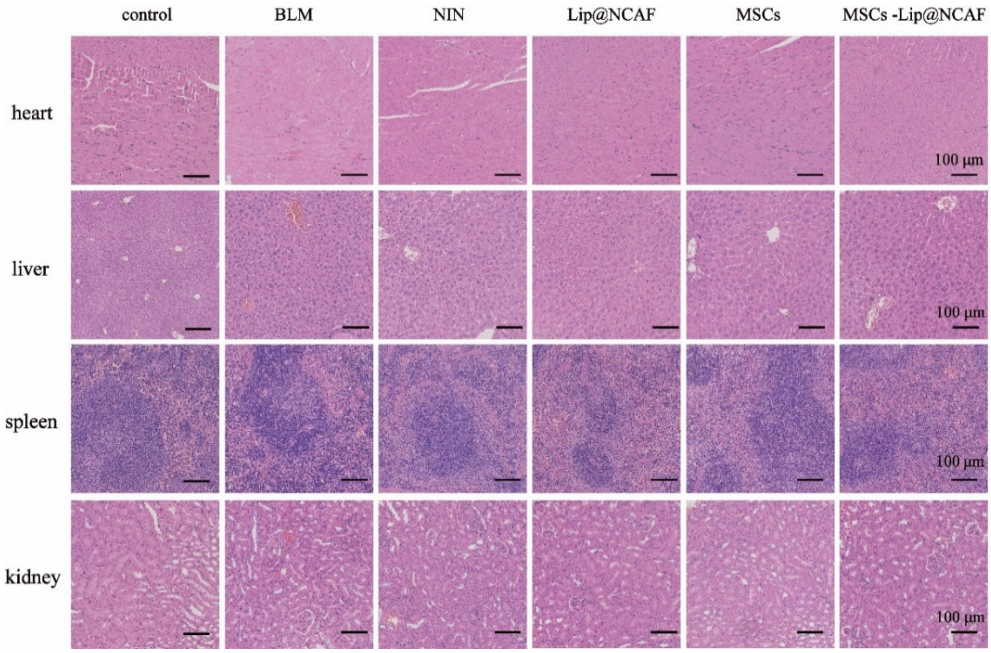

Fig. S26. Systemic toxicity after treated with different formulations. H&E staining of heart, liver, spleen and kidney of PF in aged mice treated with different formulations for 3 weeks.

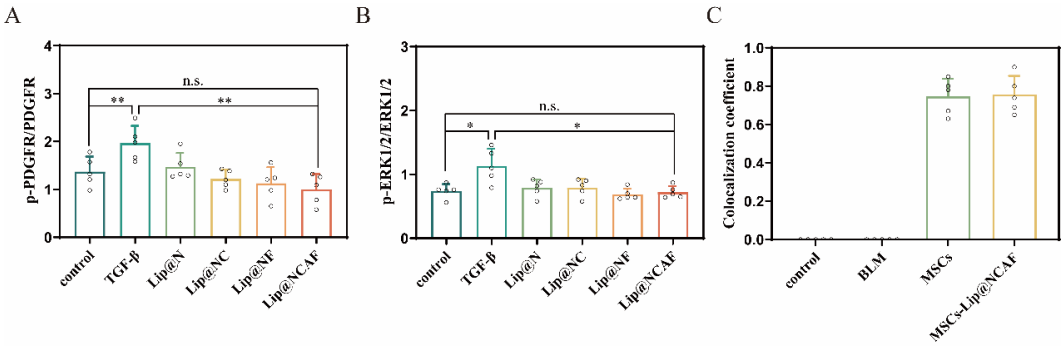

Fig. S27. Antifibrotic mechanisms of MSCs-Lip@NCAF. WB quantitative analysis of p-PDGFR (**A**) and p-ERK1/2 (**B**). (**C**) Colocalization coefficient of MSCs expressing GFP and SPC-positive AEC IIs. (n=6). Data are mean ± S.D. **P* < 0.05, ***P* < 0.01 and n.s. no significant difference.

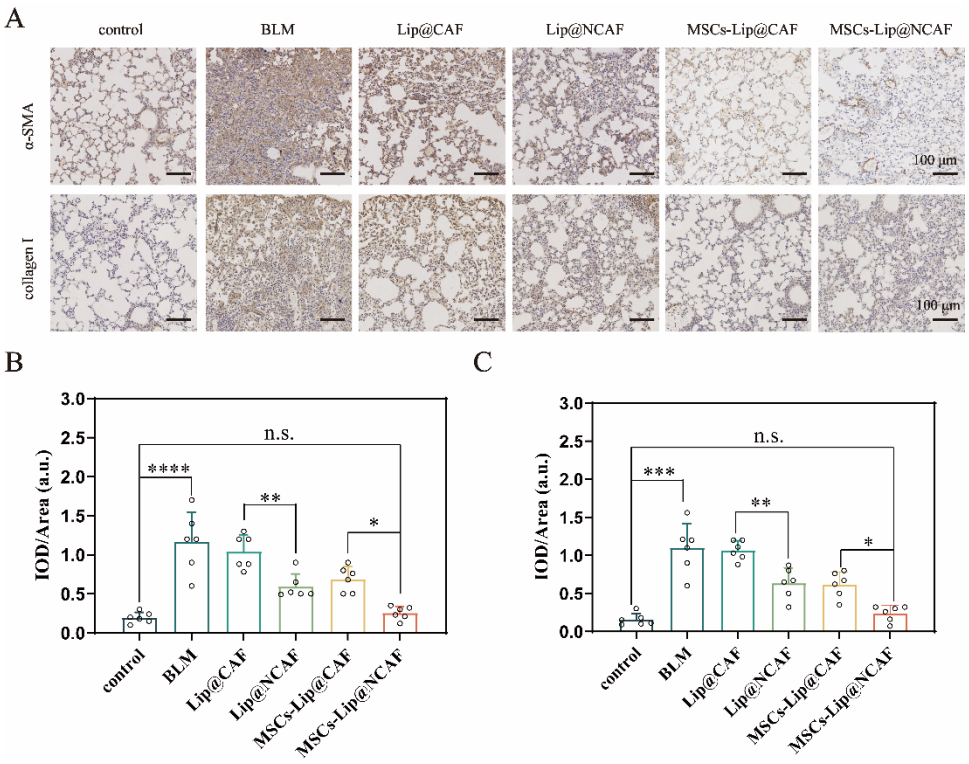

Fig. S28. The antifibrotic effects of NIN. (**A**) IHC staining of lung sections from young mice treated with different formulations. Quantitative results of α-SMA (**B**)and collagen I (**C**). (n=6). Data are means ± SD. **P* < 0.05, ***P* < 0.01, ****P* < 0.001, *****P* < 0.0001 and n.s. no significant difference.

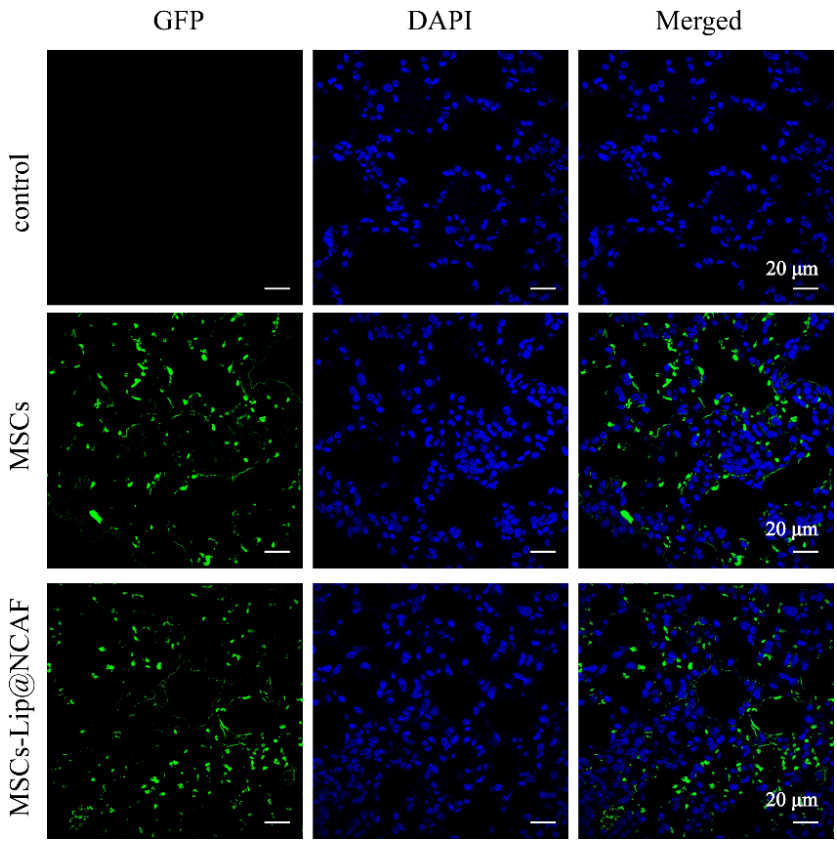

Fig. S29. The differentiation of MSCs into AEC IIs. CLSM images of lung sections from the aged mice with PF treated with MSCs and MSCs-Lip@NCAF transfected with a cell-specific expressed plasmid containing SPC promoter.

Supplementary Tables

Tab. S1. The characterization of different formulations. Size, zeta potential, EE and LC of Lip@N, Lip@NC, Lip@NF and Lip@NCAF, respectively (n=5). Data are mean ± S.D.

Formulations	Size (nm)	Zeta potential (mV)	EE (%)	LC (%)
Lip@N	82.42 ± 0.25	-2.34 ± 0.36	94.25 ± 1.26	2.23 ± 0.26
Lip@NC	85.52 ± 0.86	-2.83 ± 0.16	96.18 ± 0.47	2.41 ± 1.27
Lip@NF	84.47 ± 1.23	-3.38 ± 0.83	93.69 ± 1.42	2.51 ± 1.49
Lip@NCAF	89.25 ± 0.43	-2.76 ± 0.28	93.48 ± 0.28	2.25 ± 0.68

Tab. S2. Primer sequences of qPCR. The forward primers and reverse primers of *Col1a1*, *Sftpc*, *Fn1*, *Acta2*, *Pdgfrb*, *Cdkn2a*, *Cdkn1a*, *Mmp12*, *Mcp1*, *Gapdh*.

primer sequence	forward primer	reverse primer
Col1a1	CCTCAGGGTATTGCTGGACAAC	CAGAAGGACCTTGTTTGCCAGG
Sftpc	CATCGTTGTGTATGACTACCA	CCTGGAAGTTCTGGAGTTTTCT
Fn1	CCCTATCTCTGATACCGTTGTCC	TGCCGCAACTACTGTGATTCGG
Acta2	TGCTGACAGAGGCACCACTGAA	CAGTTGTACGTCCAGAGGCATAG
Pdgfrb	GTGGAGATTCGCAGGAGGTC	ACCGTCAGAGCTCACAGACT
Cdkn2a	CGGGGACATCAAGACATCGT	GCCGGATTTAGCTCTGCTCT
Cdkn1a	ACATCTCAGGGCCGAAAACG	AAGACACACAGAGTGAGGGC
Mmp12	GCTCCTGCCTCACATCATAC	GGCTTCTCTGCATCTGTGAA
Mcp1	AACTACAGCTTCTTTGGGACA	CATCCACGTGTTGGCTCA
Gapdh	ATGGTGAAGGTCGGTGTGAAC	GCCGTGAGTGGAGTCATACTG

Tab. S3. The primary antibodies and secondary antibodies are as follow.

Product	Supplier	Catalogue number	Dilution
Primary antibody:			
WB:			
rabbit anti-collagen I	proteintech	14695-1-AP	1: 2000
rabbit anti-fibronectin	abcam	ab2413	1: 1000
rabbit anti-α-SMA	abcam	ab5694	1: 2000
rabbit anti-SPC	abcam	ab270521	1: 1000
rabbit anti-p-PDGFR	ImmunoWay	YP0441	1: 1000
rabbit anti-PDGFR	abcam	ab203491	1: 1000
rabbit anti-p-ERK1/2	abcam	ab76299	1: 8000
rabbit anti-ERK1/2	abcam	ab184699	1: 10000
rabbit anti-β-tubulin	Beyotime	AF1216	1: 1000
IF:			
rabbit anti-collagen I	proteintech	14695-1-AP	1: 200
mouse anti-α-SMA	proteintech	67735-1-Ig	1: 500
rabbit anti-SPC	abcam	ab270521	1: 100
rabbit anti-FAP	abcam	ab218164	1: 200
rabbit anti-Vimentin	abcam	ab92547	1: 400
IHC:			
rabbit anti-collagen I	proteintech	14695-1-AP	1: 1000
mouse anti-α-SMA	proteintech	67735-1-Ig	1: 5000
Secondary antibody:			
goat anti-rabbit IgG HRP-linked Ab	Beyotime	A0208	1:1000
goat anti-rabbit IgG Alexa 647	Beyotime	A0468	1: 500

Tab. S4. Assay kits used are as follow.

Assay kit	Catalogue number	Supplier
Whole cell lysis assay kit	KGP2100	KeyGEN BioTECH
BCA protein quantitationassay kit	KGP902	KeyGEN BioTECH
Hydroxyproline assay kit	A030-2-1	Nanjing Jiancheng
Total RNA isolation kit	RE-03011	FOREGENE
All-In-One 5X RT MasterMix	G592	abm
BlasTaq™ 2X qPCR MasterMix	G891	abm
EdU assay kit	C0071S	Beyotime
TNF-α assay kit	88-7324	ThermoFisher
IL-1β assay kit	88-7013	ThermoFisher
IL-6 assay kit	88-7064	ThermoFisher
ALT assay kit	S03030	Rayto
AST assay kit	S03040	Rayto